Bioresource Technology 234 (2017) 122–130

Contents lists available at ScienceDirect

Bioresource Technology

journal homepage: www.elsevier.com/locate/biortech

Improved prediction of higher heating value of biomass using an artificial neural network model based on proximate analysis

Harun Uzun [a], Zeynep Yıldız [a], Jillian L. Goldfarb [b], Selim Ceylan [a,*]

[a] Ondokuz Mayıs University, Chemical Engineering Department, Samsun, Turkey
[b] Boston University, Department of Mechanical Engineering and Division of Materials Science & Engineering, 110 Cummington Mall, Boston, MA 02215, USA

HIGHLIGHTS

- ANN was used for forecasting higher heating values of different types of biomass.
- Proximate analysis data used for ANN model development.
- The developed ANN model was successful in predicting higher heating values.

ARTICLE INFO

Article history:
Received 20 December 2016
Received in revised form 1 March 2017
Accepted 2 March 2017
Available online 9 March 2017

Keywords:
Higher heating value
Artificial neural network
Biomass
Proximate analysis

ABSTRACT

As biomass becomes more integrated into our energy feedstocks, the ability to predict its combustion enthalpies from routine data such as carbon, ash, and moisture content enables rapid decisions about utilization. The present work constructs a novel artificial neural network model with a 3-3-1 tangent sigmoid architecture to predict biomasses' higher heating values from only their proximate analyses, requiring minimal specificity as compared to models based on elemental composition. The model presented has a considerably higher correlation coefficient (0.963) and lower root mean square (0.375), mean absolute (0.328), and mean bias errors (0.010) than other models presented in the literature which, at least when applied to the present data set, tend to under-predict the combustion enthalpy.

1. Introduction

As our society ponders the consequences of global climate change and decreasing fossil fuel resources, researchers worldwide are searching for renewable fuels that are economically viable, technologically feasible, and environmentally sustainable. The last of these qualifications – sustainability – has evolved to include developing fuels from raw materials that are locally sourced to avoid long-range transport; that do not compete with land and water used for food and fiber production; and that reduce net greenhouse gas emissions (Singh et al., 2011). As a result, the potential for biomass to serve as a sustainable supply of energy has become a major research topic all over the world.

However, the design of new systems that integrate electricity, heat and transport fuels from biomass, biomass and geothermal sources (Malik et al., 2015) and biomass conversions with CO_2 capture and utilization (Sharifzadeh et al., 2015) require knowledge of the fundamental characteristics of the biomass, especially its higher heating value (HHV). Such properties are critical to the design and operation of biomass combustion systems (Ghugare et al., 2014). Furthermore, to determine the conversion efficiency of the biological or thermochemical conversion of biomass to energy, the potential energy content of biomass must be known (McKendry, 2002). The HHV of a fuel is equal to the amount of heat released when a unit mass of the fuel is burnt completely, accounting for the enthalpy of condensation of liquid water as a combustion product under standard conditions. Fuels with higher HHVs will have the highest possible energy output (Xu and Yuan, 2015).

The HHV of a candidate biomass fuel can be experimentally evaluated using an adiabatic oxygen bomb calorimeter, a simple and accurate measurement of the changes between a reactant and products' enthalpy. Despite its simplicity, it may not always be feasible to analyze the HHV experimentally (Callejón-Ferre et al., 2014). There are many models that correlate the elemental composition (C, H, N, O, S) of solid fuels and the HHV, including coal (Mason and Gandhi, 1983); municipal solid waste (Kathiravale et al., 2003), and more recently, biomass (Erol et al., 2010; Friedl et al., 2005; Nhuchhen and Salam, 2012; Shen et al., 2010). However, elemental analysis can be costly and time

* Corresponding author.
E-mail address: selim.ceylan@omu.edu.tr (S. Ceylan).

http://dx.doi.org/10.1016/j.biortech.2017.03.015
0960-8524/

consuming, such that researchers are turning towards empirical methods to predict the HHV of solid fuels such as biomass using proximate analysis data alone (Cordero et al., 2001; Parikh et al., 2005). Such mathematical models are based on the weight percentages (wt.%) of moisture, volatile matter (VM), fixed carbon (FC) and ash of the solid fuel.

Artificial neural network (ANN) modeling is an emerging tool for the description of biodiesel stability, centane number and conversion rates based on fuel properties (Filho et al., 2015; Ramadhas et al., 2006), and to predict how fuel and fuel blends behave in thermal conversion scenarios (De et al., 2007; Guo et al., 2001). ANNs have been used quite broadly to model experimental results across the scientific literature, from modeling treatment of water pollutants (Maurya et al., 2014), to pattern recognition in chromatographic spectra for food analysis and genomic and proteomic sequences (Almeida, 2002; Chen et al., 2008) to process systems modeling such as mycelial fermentation processes, product compositions after distillations, and predictive failure control (Willis et al., 1991). These mathematical tools are so widely applied because of their inherent versatility in connecting single processing elements – known as nodes or neurons – in parallel computation to both process and represent knowledge (Basheer and Hajmeer, 2000). These neurons are combined in a nonlinear transfer function to yield a final result in terms of weights and biases (Vani et al., 2015). ANNs have the ability to learn mathematical models through experience – learning from the functionality of the network – without the need to explicitly determine the mathematical relationships that tie together the nodes' interrelated solutions. The Artificial Neural Network is thus not a programmed model, but rather a trained system based on empirical data (Buratti et al., 2014). Empirical models constructed from artificial neural networks are increasingly used because of their predictive capability and accuracy, even for small datasets.

There are a handful of examples in the literature of researchers using ANNs to predict the HHV of solid fuels. For example, Mesroghli et al. (2009) employed a nonlinear ANN model for estimation of the HHV of coals. Channiwala and Parikh (2002) proposed a unified correlation to predict HHV from elemental analysis of fuels in the solid, liquid and gas phases, from fossil and biomass sources, and raw, char, and residue-derived fuels. Using seven nonlinear models, Patel et al. (2007) estimated the HHV of coals. Friedl et al. (2005) used a set of 122 plant material samples to develop regression models to predict HHV from the biomass' elemental compositions. Likewise, Ghugare et al. (2014) focused on predicted HHV of solid biomasses via a multilayer perceptron neural network as well as genetic programming-based models, with ultimate analysis an essential part of their correlations.

Such prediction methodologies, while accurately representing HHV, often rely on the ultimate or ultimate plus proximate analyses of the raw fuels. Oftentimes, the ultimate analysis is not available. Conversely, the proximate analysis of a solid fuel, including moisture (M), volatile matter (VM), ash (A) and fixed carbon (FC), is easily determined (Callejón-Ferre et al., 2014), and considerably more cost and time effective than ultimate analyses. In addition, the ability to "design" a fuel or fuel mixture could be significantly improved by being able to quickly predict the HHV based on such simple factors as moisture, volatile matter, fixed carbon, and ash. For example, Haykiri-Acma et al. (2015) demonstrated that the fuel segregation in biomass-coal blends can be reduced or eliminated by carbonization of the biomass, increasing the HHV and heating density. Similarly, Goldfarb and Liu (2013) found that HHV is linearly related to the percent, by mass, of torrefied biomass in a mixture with coal. Thus, the ability to swiftly predict the HHV of a fuel – or fuel mixture – could inform decisions about pre-processing of coal based on volatile and fixed matter targets.

The present study is focused on the development of a correlation for predicting the HHV of solid fuels from only their proximate analyses to remove the need for time-consuming and expensive ultimate analyses in making such predictions. Building off of the success of previous models to use proximate analyses to predict elemental composition, and elemental composition to predict HHV, the present work demonstrates the possibility of using proximate analyses to directly predict HHV. In this paper, a new approach using artificial neural networks modeling is proposed, developed, and analyzed for forecasting errors. 131 published data points of higher heating values for biomasses ranging from 10.14 MJ/kg to 21.78 MJ/kg are used to develop the model. The model was validated using experimentally determined higher heating values of biomass, and the correlations are compared to other published correlations.

2. Materials and methods

2.1. Collection of data

Proximate analyses results and HHVs collected from the literature for various types of biomass species are presented in Table 1. The biomasses represented in the database vary from agricultural wastes (e.g. rice husk and corn straw) to forest residue (e.g. willow and oak wood) to sewage sludge. For all 131 biomass samples in the training set, the volatile matter (VM), FC (fixed carbon) contents, and HHV were within 60–90 wt.%, 35–55 wt.% and 14–23 MJ/kg, respectively. This dataset represents one of the most diverse biomass sources used for HHV modeling in the literature, to date.

2.2. Artificial neural network architecture and evaluation

To model complex systems, artificial neural networks (ANN) use interconnected mathematical "neurons," or "nodes," to create a structure. The input signals – of varying intensity and strength – feed through the neuron, and combine to form a net input into another neuron. The output layer, equal to the number of dependent variables, is calculated by weight and bias associated with connections among neurons. ANNs are organized into layers of an *l*-*m*-*n* structure with *l* neutrons at the input layer (number of model inputs), *m* neurons at the hidden layer (in this case, experimentally optimized) and *n* neurons in the output (depending on desired outputs) (Giri et al., 2011). The hidden node calculates the weighted sum of all the inputs, W_{ji}, or the interconnection of the ith node of the first layer to the jth node of the second layer. The sum of the modified signals is then transformed via a nonlinear transfer function, $f_{(net)}$, to determine the node's output. In this study we probe both tangential and logistic sigmoid transfer functions for $f_{(net)}$.

The sigmoid transfer function is a bounded, monotonic, nondecreasing, S-curve of a nonlinear response (Giri et al., 2011). For any variable x, it takes the form:

$$f(x) = \frac{1}{1 + e^{-x}} \tag{1}$$

The tangential sigmoid transfer function assumes the form:

$$f(x) = \frac{2}{1 + e^{-2x}} - 1 \tag{2}$$

In this study, ANN modeling was performed using Matlab 7.9.0 mathematical software using the ANN toolbox. To train the model, the proximate analysis databases were partitioned in training and test sets using an 67:33 train:test ratio. Accordingly, the dataset for the proximate analysis-based modeling contained 88 training, and 43 test data points, the latter of which were used for validation of

Table 1
Proximate and HHV literature values used in ANN model construction.

Biomass materials	Proximate Analysis (% by wt. dry basis)			Measured HHV (Mj/kg)	Reference
	FC[a]	VM[b]	ASH		
Sludge C5	5.96	42.25	51.79	10.14	Thipkhunthod et al. (2005)
Sludge C4	4.05	47.58	48.37	11.02	Thipkhunthod et al. (2005)
Sludge H3	6.47	47.68	45.86	12.39	Thipkhunthod et al. (2005)
Sludge C3	6.99	49.98	43.03	12.56	Thipkhunthod et al. (2005)
Sludge H2	6.84	52.57	40.60	12.77	Thipkhunthod et al. (2005)
Sludge C2	6.73	51.24	42.03	13.18	Thipkhunthod et al. (2005)
Sludge H1	5.14	55.47	39.39	13.34	Thipkhunthod et al. (2005)
Sludge C1	8.61	53.01	38.38	13.92	Thipkhunthod et al. (2005)
Coal sample	30.00	30.00	40.00	14.77	Parikh et al. (2005)
Water hyacinth	1.90	87.30	10.80	14.81	Parikh et al. (2005)
Rice hulls	15.80	63.60	20.60	14.89	Nhuchhen and Salam (2012)
Tobacco leaf	11.20	72.60	17.20	15.00	Demirbaş (1997)
Rice straw	15.86	65.47	18.67	15.09	Yin (2011)
Mentha Piperita	7.50	79.00	13.50	15.15	Parikh et al. (2005)
Eucatlyptus bark	15.30	65.70	19.00	15.20	Parikh et al. (2005)
Rice husk bran	19.53	61.83	18.64	15.29	Channiwala and Parikh (2002)
Spire-mint	11.80	70.10	18.10	15.53	Parikh et al. (2005)
Rice straw (ground)	16.20	68.30	15.50	15.61	Parikh et al. (2005)
Rice husk patni-23	14.90	69.30	15.80	15.67	Channiwala and Parikh (2002)
Cotton stalks	19.90	62.90	17.20	15.83	Channiwala and Parikh (2002)
Sun flower stalk and stover	5.17	85.85	8.98	15.87	Küçükbayrak et al. (1991)
Bamboo dust	9.30	74.20	16.50	15.89	Parikh et al. (2005)
Cotton shells	16.90	68.50	14.60	16.38	Parikh et al. (2005)
Sludge sample 1	9.80	60.70	29.50	16.60	Thipkhunthod et al. (2005)
Rapeseed	5.60	86.27	8.13	16.61	Küçükbayrak et al. (1991)
Pine wood	15.70	73.60	11.30	16.64	Parikh et al. (2005)
Sludge sample 4	9.70	59.30	31.00	16.80	Thipkhunthod et al. (2005)
Wheat straw	23.50	63.00	13.50	17.00	Demirbaş (1997)
Hybrid poplar	6.87	89.69	3.44	17.14	Küçükbayrak et al. (1991)
Potato peel	9.56	84.15	6.29	17.18	Küçükbayrak et al. (1991)
Sugar cane straw	14.60	76.20	9.20	17.19	Suárez et al. (2000)
Sugarcane	14.95	73.78	11.27	17.33	Nhuchhen and Salam (2012)
Bagasse	14.95	73.78	11.27	17.33	Channiwala and Parikh (2002)
Wheat straw	11.70	80.60	7.70	17.36	Parikh et al. (2005)
Sudan Grass	18.60	72.75	8.65	17.39	Parikh et al. (2005)
Sugar cane leaves	14.90	77.40	7.70	17.41	Parikh et al. (2005)
Cotton cake	11.58	83.65	4.77	17.50	Küçükbayrak et al. (1991)
Wheat straw	19.80	71.30	8.90	17.51	Nhuchhen and Salam (2012)
Sour cheery stone	14.10	80.85	5.05	17.59	Küçükbayrak et al. (1991)
Bamboo stick waste	47.70	12.70	39.60	17.66	Parikh et al. (2005)
Corn straw	19.19	73.15	7.65	17.68	Masiá et al. (2007)
Sugarcane bagasse	13.30	81.50	5.20	17.70	Munir et al. (2009)
Streeter tall wheatgrass	18.20	73.80	8.00	17.90	Nhuchhen and Salam (2012)
Eucalyptus log	8.05	82.78	0.37	17.99	Nhuchhen and Salam (2012)
Millet straw	16.45	78.28	5.27	18.05	Channiwala and Parikh (2002)
Ash tree	14.12	80.13	5.75	18.06	Küçükbayrak et al. (1991)
Streeter switch grass	17.70	76.50	5.80	18.06	Nhuchhen and Salam (2012)
Streeter intermediate wheatgrass	17.90	74.40	7.80	18.08	Nhuchhen and Salam (2012)
Bagasse	11.90	86.30	1.80	18.17	Parikh et al. (2005)
RDF	14.31	81.22	4.48	18.19	Nhuchhen and Salam (2012)
Cotton stalk	22.43	70.89	6.68	18.26	Nhuchhen and Salam (2012)
Soybean cake	16.00	76.86	7.14	18.30	Küçükbayrak et al. (1991)
Rape straw	17.81	76.54	4.65	18.34	Masiá et al. (2007)
Carrington switch grass	18.70	76.60	4.80	18.45	Nhuchhen and Salam (2012)
Casuarina equisetifolia leaf	16.46	73.50	3.93	18.48	Sugumaran and Seshadri (2009)
Apricot bagasse	15.80	80.31	3.89	18.56	Küçükbayrak et al. (1991)
Peanut shell	13.40	84.90	1.70	18.60	Bonelli et al. (2003)
Chaparral wood	18.68	75.19	6.13	18.61	Channiwala and Parikh (2002)
Eucalyptus	21.30	75.35	3.35	18.64	Parikh et al. (2005)
Alfalfa stems	15.81	78.92	5.27	18.67	Jenkins et al. (1998)
Olive twigs	10.73	88.25	1.02	18.70	Jiménez and González (1991)
Sugarcane bagasse	13.15	83.66	3.20	18.73	Channiwala and Parikh (2002)
Casurina wood	19.58	78.58	1.83	18.77	Channiwala and Parikh (2002)
Corncob	18.54	80.10	1.36	18.77	Parikh et al. (2005)
Corn cob	16.80	82.10	1.10	18.80	Parikh et al. (2005)
Apricot stone	17.83	81.13	1.04	18.80	Küçükbayrak et al. (1991)
Almond hulls	20.07	73.80	6.13	18.89	Jenkins et al. (1998)
Wheat straw	24.00	69.60	6.40	18.91	Parikh et al. (2005)
Walnut shell	16.94	79.17	3.89	18.91	Küçükbayrak et al. (1991)
Industrial waste (stalla)	20.10	75.10	4.80	18.93	Parikh et al. (2005)
Tan Oak	9.20	90.60	0.20	18.93	Parikh et al. (2005)
Ply wood	15.77	82.14	2.09	18.96	Channiwala and Parikh (2002)
Canyon live Oak	11.30	88.20	0.50	18.98	Parikh et al. (2005)

Table 1 (*continued*)

Biomass materials	Proximate Analysis (% by wt. dry basis)			Measured HHV (Mj/kg)	Reference
	FC[a]	VM[b]	ASH		
Olive husk	26.10	70.30	3.60	19.00	Demirbaş (1997)
Miscanthus pellet	17.40	80.21	2.37	19.00	Nhuchhen and Salam (2012)
Cornelian cherry stone	23.80	73.54	2.96	19.02	Küçükbayrak et al. (1991)
Hybrid poplar	12.49	84.81	2.70	19.02	Jenkins et al. (1998)
Cabernet Sauvignon	19.20	78.63	2.17	19.03	Parikh et al. (2005)
Cotton shells briquettes	17.10	77.80	5.10	19.06	Parikh et al. (2005)
Eucalyptus stalk	12.20	87.30	0.50	19.10	Parikh et al. (2005)
Esparto plant	16.80	80.50	2.20	19.10	Debdoubi et al. (2005)
Oak wood (large branch)	16.18	81.75	2.07	19.17	Miranda et al. (2009)
Oak wood (small branch)	18.50	77.45	4.05	19.20	Miranda et al. (2009)
Alabama Oak wood waste	21.90	74.70	3.30	19.23	Parikh et al. (2005)
Eucalyptus globulus wood	17.30	81.60	1.10	19.23	Channiwala and Parikh (2002)
Oak wood (medium branch)	16.18	80.82	3.00	19.24	Miranda et al. (2009)
Pistachio shell	16.84	82.03	1.13	19.26	Parikh et al. (2005)
Miscalthus (elephanta grass)	12.40	87.20	0.40	19.30	Parikh et al. (2005)
Red alder	12.50	87.10	0.40	19.30	Nhuchhen and Salam (2012)
Eucalyptus-Grandis	16.93	82.55	0.52	19.35	Parikh et al. (2005)
Poplar	16.35	82.32	1.33	19.38	Nhuchhen and Salam (2012)
White oak	17.20	81.28	1.52	19.42	Nhuchhen and Salam (2012)
Eucalyptus camaldulensis	17.82	81.42	0.76	19.42	Nhuchhen and Salam (2012)
Peach Pit	19.80	79.10	1.10	19.42	Parikh et al. (2005)
Coconut stem	23.10	74.40	2.50	19.44	Parikh et al. (2005)
Almond shells	20.71	76.00	3.29	19.49	Yin (2011)
Forest residue	20.00	79.80	0.20	19.50	Vamvuka et al. (2003)
Madrone	12.00	87.80	0.20	19.51	Nhuchhen and Salam (2012)
Peach stone	20.79	78.16	1.05	19.52	Küçükbayrak et al. (1991)
Willow wood	16.07	82.22	1.71	19.59	Jenkins et al. (1998)
Coconut shell powder	20.58	79.07	0.35	19.68	Parikh et al. (2005)
Fresh subabul wood	15.20	83.60	1.12	19.70	Channiwala and Parikh (2002)
Black locust	18.26	80.94	0.80	19.71	Nhuchhen and Salam (2012)
Ply wood	21.80	74.20	4.00	19.72	Parikh et al. (2005)
Subabul wood	18.52	81.02	1.20	19.78	Parikh et al. (2005)
Shea meal	28.70	66.30	5.00	19.80	Munir et al. (2009)
Coffee husk	19.10	78.50	2.40	19.80	Suárez et al. (2000)
Black walnut pruning	18.56	80.69	0.78	19.83	Nhuchhen and Salam (2012)
Tea bush	21.80	76.50	1.70	19.84	Parikh et al. (2005)
Olive kernel	24.25	73.62	2.13	19.90	Vamvuka et al. (2003)
Wood Chips	23.50	76.40	0.10	19.92	Parikh et al. (2005)
Almond shell	18.40	80.50	1.10	19.92	Cordero et al. (2001)
White Fir	16.58	83.17	0.25	19.95	Parikh et al. (2005)
Walnut	20.80	78.50	0.70	19.97	Parikh et al. (2005)
Softwood	28.10	70.00	1.70	20.00	Demirbaş (1997)
Akhrot shell	18.78	79.98	1.20	20.01	Channiwala and Parikh (2002)
Almond	21.54	76.83	1.63	20.01	Parikh et al. (2005)
Ponderosa pine	17.17	82.54	0.29	20.02	Nhuchhen and Salam (2012)
B-wood	21.62	76.53	1.85	20.05	Yin (2011)
Coconut coir	29.70	66.58	3.72	20.05	Parikh et al. (2005)
Es	17.90	82.00	0.10	20.08	Cordero et al. (2001)
Spruce wood	28.30	70.20	1.50	20.10	Demirbaş (1997)
Pine needles	26.12	72.38	1.50	20.12	Nhuchhen and Salam (2012)
Walnuts shells	21.16	78.28	0.56	20.18	Nhuchhen and Salam (2012)
Wood bark	31.80	66.60	1.60	20.50	Demirbaş (1997)
Coconut shell	22.10	77.19	0.71	20.50	Channiwala and Parikh (2002)
Ceder cones	28.10	70.40	1.50	21.10	Parikh et al. (2005)
Olive kernel shell	36.10	60.50	3.30	21.40	Demirbaş and Ilten (2004)
Olive cake	34.60	62.10	2.80	21.60	Demirbaş and Ilten (2004)
Loblolly Pine	33.90	65.70	0.40	21.77	Parikh et al. (2005)
Loblolly pine bark	33.90	54.70	0.40	21.78	Nhuchhen and Salam (2012)

[a] Fixed Carbon.
[b] Volatile Matter.

the model. Defining the number of neurons in the hidden layer is a field of study unto itself, based on an equilibrium between convergence and generalization that insures accuracy without increasing complexity unnecessarily. Kolmogorov's Mapping Neural Network Existence Theorem suggests that with the hidden layer should have $2l + 1$ neurons (Gupta et al., 2004), whereas the Rule of Thumb suggests that the number of hidden neurons, m, is a function of the number of training samples, N_{train} (Principe et al., 2000):

$$m = \left(\frac{N_{train}}{10} - l\right)\frac{1}{l+n+1} \quad (3)$$

In this paper, the number of neurons in the hidden layer was calculated by trial and error to minimize mean square error of the models. The trial and error approach, as will be shown, led to some models with architectures too large to be practical according to such rules of thumb. However, the model "fits" to lower level, more suitable architectures, were actually superior; this is discussed in the Section 3.

To insure a homogeneous distribution of data (to select the training versus testing sets) data were put in increasing order of HHV, and every 3rd dataset was selected for testing. To prevent overtraining of the ANN, when preliminary results showed a con-

stant MSE after a given iteration number; this iteration was selected as the stop criteria and added into the MATLAB code. Fig. 1 is a schematic representation of the architecture of the multilayer ANN used in this investigation

The ANN models were evaluated using the root mean square error (RMSE) between actual and predicted measurements as:

$$RMSE = \sqrt{\frac{1}{N}\sum_{i=1}^{N}(H_i - H_{i,model})^2} \quad (4)$$

where H is the higher heating value of a given biomass and its model prediction, respectively, and N is the number of observations. The mean absolute error (MAE) was calculated as:

$$MAE = \frac{1}{N}\sum_{i=1}^{N}|H_i - H_{i,model}| \quad (5)$$

and the mean bias error (MBE) as:

$$MBE = \frac{1}{N}\sum_{i=1}^{N}(H_i - H_{i,model}) \quad (6)$$

3. Results and discussion

Artificial neural network modeling is a sophisticated tool to enable the scientist to understand multiple, nonlinear contributions of a set of properties or variables on a determinant variable. To gauge the appropriateness of linear or nonlinear relationships for biomass HHV prediction, individual constituents of the proximate analyses were plotted against the corresponding HHVs. As shown in Fig. 2, there exists at best a loosely linear relationship between the HHV and percentages of carbon, fixed carbon, and ash, but not satisfactory for any meaningful HHV predictions. It is thus inferred that linear models may not represent the most appropriate solution to accurately predict biomass HHV. As such, we actively pursue nonlinear models. Of course, the complexity in this situation is in determining the exact form the proximate analysis-based nonlinear empirical model to predict biomass HHV should take. This challenge can be overcome using artificial intelligence based data-driven modeling in the form of ANNs.

3.1. ANN model for HHV prediction

This study probed the applicability of 78 different ANN models with various network structures using both tangent and logistic sigmoid hidden layer transfer functions, all with linear output layers. Model performance was evaluated by considering the root mean squared error (RMS), mean bias error (MBE) and mean absolute error (MAE) and via correlation coefficients between predicted and actual HHV values. Overall, 15 of the 78 tested models had RMSE less than 0.500; these models are presented in Table 2 (all 78 models presented in the Supplemental Information.) Of these, 12 had correlation coefficients greater than 0.93, with only 2 greater than 0.91 (ANN 13, 24). ANN 13, a 3-3-1 tangent sigmoid model, had a lower RMSE (0.375 vs. 0.392), lower MBE (0.328 vs. 0.344) and lower MAE (0.010 vs. 0.016), and a considerably smaller network structure than ANN 24, with a 3-20-1 structure. ANN 13 relies on a set of three tangent sigmoid equations with inputs of FC, VM and Ash composition as the first layer. The second also has three tangent sigmoid equations that use the results of the first node as inputs into this layer. Finally, the third layer uses the numerical results of the three second layer equations to determine HHV. The coefficients and equations of each node are provided in the Supplemental Information. Examining Fig. 3, the ANN predicted versus measured HHV plots, there is minimal bias in the model's prediction. Residual errors appear to both under and over-predict HHV values at similar rates. Such an architecture is in general agreement with ANN Rules of Thumb for the total number of hidden layer notes as calculated by Eq. (3), which would suggest, with three input layers and 131 data points for training, a 3-(2.42)-1 architecture.

One might expect the ability to model HHVs using only proximate analysis to be hampered by lack of specificity in terms of elemental composition. Certainly breaking C–C vs. C–H bonds yield different quantities of energy that on the outset might not be captured by a proximate analysis prediction. However, the success of the present ANN model using only proximate analysis to predict HHV is underscored by the previously demonstrated ability to predict elemental composition from proximate analysis as presented by Parikh et al. (2007). Their model was able to predict elemental composition for a variety of biomass materials for C, H and O with

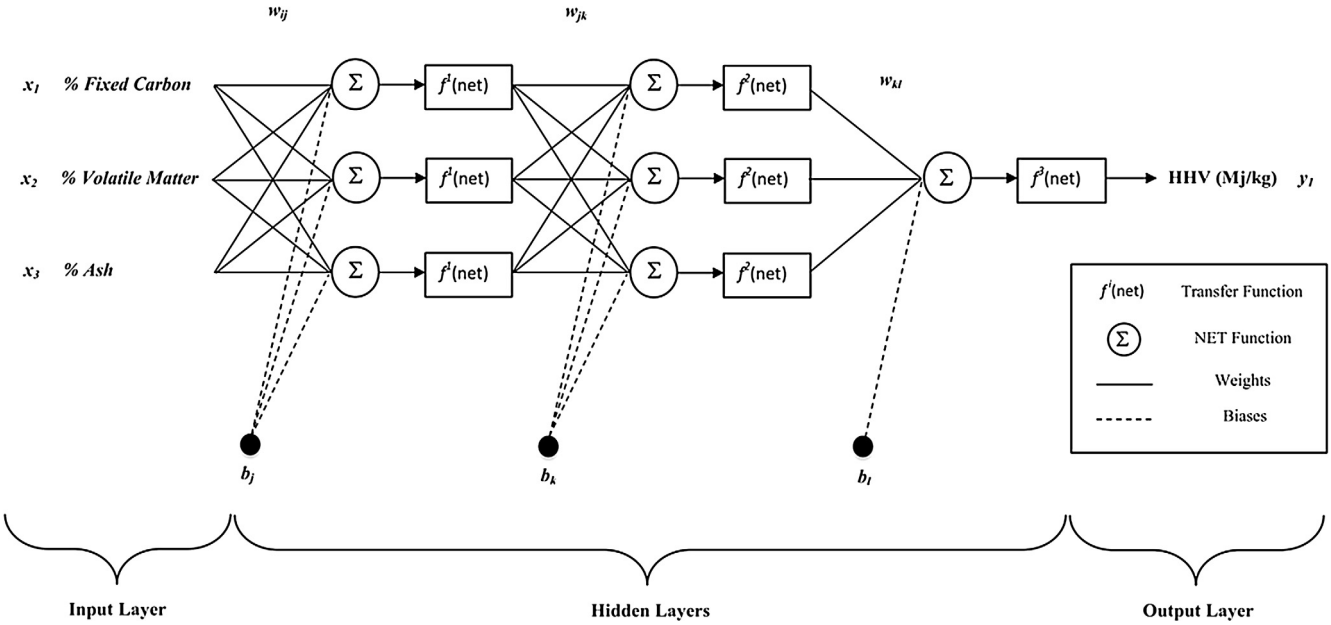

Fig. 1. Schematic representation of ANN using proximate analysis data to predict HHV of solid fuels.

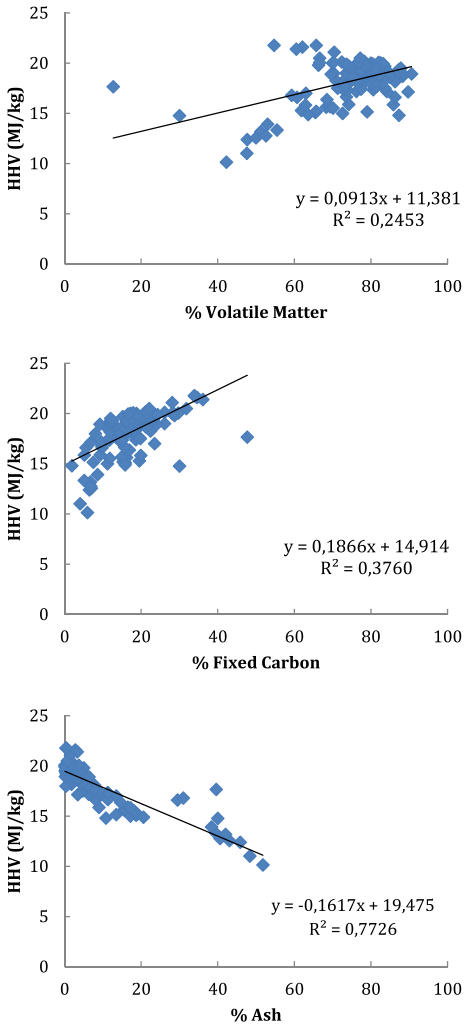

Fig. 2. Relationships between HHV and individual constituents of proximate analyses.

less than 5% average absolute error. As such, we might expect that if proximate analysis can "back predict" elemental composition, it is suitable for predicting the HHV resulting from the breaking of these bonds.

3.2. Comparison of ANN model to prior literature models predicting HHV

In Fig. 3, the predicted versus actual HHV values from the ANN 13 model proposed here are compared alongside four models available in the literature that use varying methods to predict HHV. From these plots, we can see that the ANN13 model has the highest correlation coefficients and best predictive capability. This is underscored by the considerably higher errors as presented in Table 3 for other models' predictions. The Ghugare et al. (2014) model shows the best predictive capabilities of the four models investigated, with the highest correlation coefficient (0.934) and lowest RMSE and MAE (0.508 and 0.285, respectively). However, this model has a tendency to under-predict the HHVs, as seen by an MBE of −0.119.

In the various models available in the literature to predict HHV from proximate and/or ultimate analyses, one feature that limits their widespread applicability is the range of biomasses used to either determine correlations or train a model. For example, Yin (2011) generated an empirical correlation for the prediction of HHV from both proximate and ultimate analyses of biomass with a mean absolute error of less than 5%. However, their data set comprised biomasses that were predominantly nut/seed shells, fruit stones, straws/grasses, and wood. However, Nhuchhen and Salam (2012) expanded a data set to include a variety of agricultural wastes, food waste, and sludge samples, as we have done in the present work. Given the greater variety of the biomass represented by Nhuchhen and Salam (2012), it is not surprising that their correlations based on linear relationships between proximate analysis and HHV suffered mean absolute errors of at least 9% and higher, and absolute bias errors of up to 4.5%. Their study proposed 20 new correlations between FC, VM, and Ash to predict HHV, however they are linear functions of two and/or three of these biomass descriptors, and as we previously demonstrated in Fig. 2, the relationships among these variables is not expected to be linear. However, this study used a "propose and test" method, where each correlation was proposed and corresponding coefficients calculated, then errors determined. In the present study, rather than propose and test correlations using such a brute force method, we turned to computational modeling to train a neural network model to provide a new correlation with improved predictive capabilities over models previously available in the literature.

Table 2
Selected ANN models with RMSE less than 0.500 (all model results available in Supplemental Information).

Model name	Network	Transfer functions		RMSE	MAE	MBE	CC
		Hidden layer	Output layer				
ANN13	3-3-1	Tangent Sigmoid	Linear	0.375	0.328	0.010	0.963
ANN24	3-20-1	Logistic Sigmoid	Linear	0.392	0.344	−0.016	0.962
ANN8	7-1	Logistic Sigmoid	Linear	0.439	0.369	−0.064	0.958
ANN38	5-20-1	Logistic Sigmoid	Linear	0.413	0.352	0.054	0.953
ANN25	3-25-1	Tangent Sigmoid	Linear	0.419	0.347	−0.003	0.953
ANN6	5-1	Logistic Sigmoid	Linear	0.416	0.353	−0.041	0.952
ANN16	3-5-1	Logistic Sigmoid	Linear	0.451	0.367	−0.075	0.950
ANN36	5-15-1	Logistic Sigmoid	Linear	0.454	0.382	0.015	0.944
ANN5	5-1	Tangent Sigmoid	Linear	0.471	0.413	−0.025	0.939
ANN14	3-3-1	Logistic Sigmoid	Linear	0.484	0.411	−0.041	0.938
ANN27	3-30-1	Tangent Sigmoid	Linear	0.479	0.411	−0.046	0.936
ANN43	7-7-1	Tangent Sigmoid	Linear	0.413	0.159	−0.065	0.749
ANN45	7-10-1	Tangent Sigmoid	Linear	0.334	0.181	0.007	0.724
ANN23	3-20-1	Tangent Sigmoid	Linear	0.419	0.201	−0.037	0.636
ANN42	5-30-1	Logistic Sigmoid	Linear	0.470	0.264	−0.069	0.466

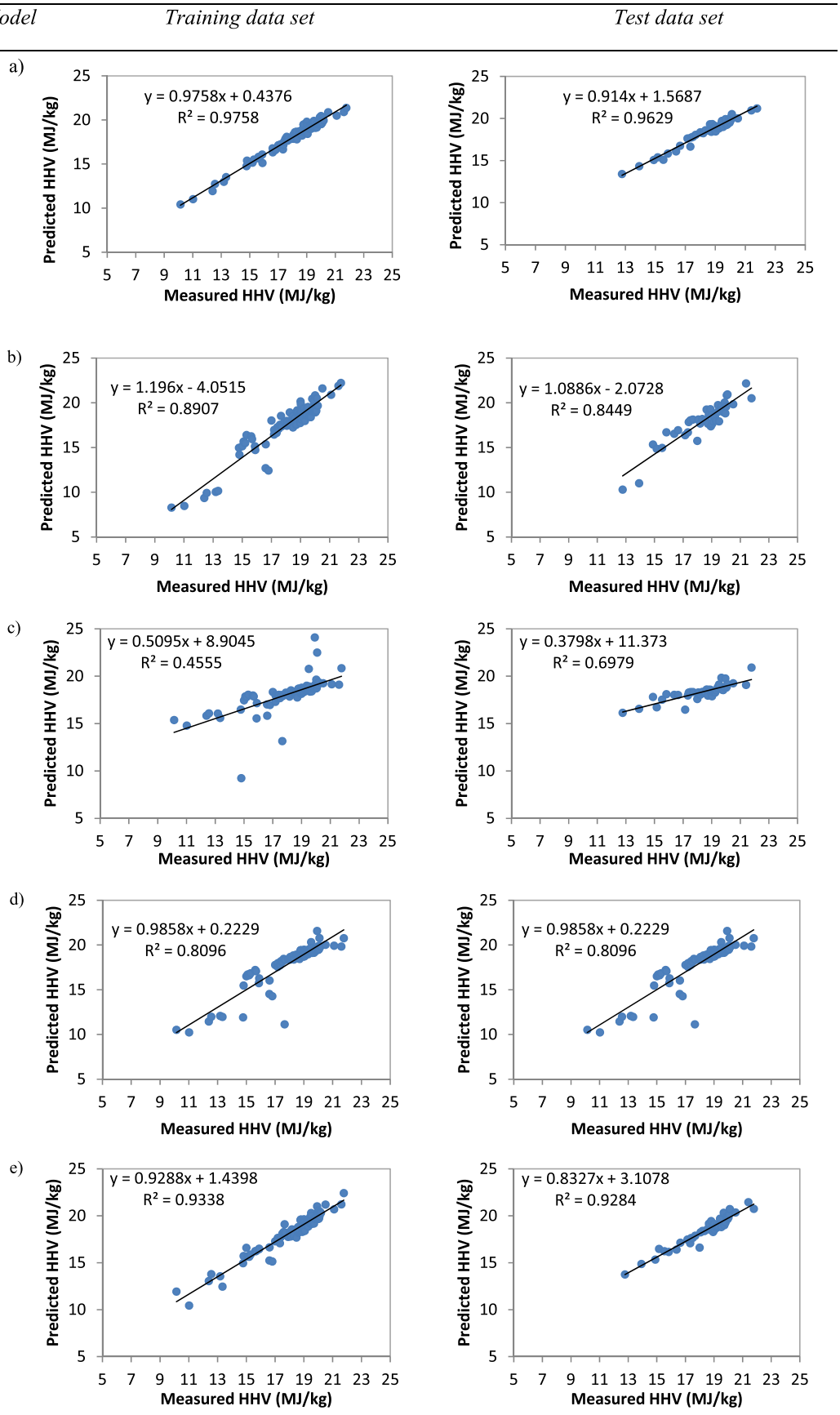

Fig. 3. Plots of calculated HHVs from test and training data using different models a) ANN13 (this study) b) Parikh et al. (2005) c) Nhuchhen and Salam (2012) d) Nhuchhen and Salam (2012) e) Ghugare et al. (2014).

Table 3
Results of ANN13 as compared to published literature models for biomass training and testing set.

Model	Training Set				Testing Set			
	[a]RMSE	[b]MAE	[c]MBE	[d]CC	[a]RMSE	[b]MAE	[c]MBE	[d]CC
ANN13 (this study)	0,219	0,121	−0,022	0,976	0,375	0,328	0,010	0,963
Parikh et al. (2005)	1,043	0,502	0,359	0,891	1,000	0,780	0,446	0,845
Nhuchhen and Salam (2012)	1,431	0,679	−0,354	0,456	1,260	0,997	0,012	0,698
Nhuchhen and Salam (2012)	0,997	0,464	−0,016	0,810	0,675	0,548	−0,098	0,880
Ghugare et al. (2014)	0,508	0,285	−0,119	0,934	0,539	0,426	−0,036	0,928

[a] Root Mean Squared Error.
[b] Mean Absolute Error.
[c] Mean Bias Error.
[d] Correlation Coefficient.

4. Conclusion

The ability to accurately predict the higher heating value of carbonaceous biomasses from knowledge of proximate analysis alone could help transform the way we select biomass feedstocks, and their blends, for renewable fuel applications. In this work, we used a dataset of 131 biomass samples to build an artificial neural network model to predict HHV based only on fixed carbon, volatile carbon, moisture and ash contents. The resulting model is a 3-3-1 tangent sigmoid model with a higher correlation coefficient and lower root mean square, mean absolute, and mean bias errors than other correlations presently available in the literature.

Acknowledgement

This study was supported by Ondokuz Mayıs University/BAP with a project number PYO.MUH. of 1904.15.012.

Appendix A. Supplementary data

Supplementary data associated with this article can be found, in the online version, at http://dx.doi.org/10.1016/j.biortech.2017.03.015.

References

Almeida, J.S., 2002. Predictive non-linear modeling of complex data by artificial neural networks. Curr. Opin. Biotechnol. 13, 72–76.
Basheer, I.A., Hajmeer, M., 2000. Artificial neural networks: fundamentals, computing, design, and application. J. Microbiol. Methods 43, 3–31.
Bonelli, P.R., Cerrella, E.G., Cukierman, A.L., 2003. Slow pyrolysis of nutshells: characterization of derived chars and of process kinetics. Energy Sources 25, 767–778.
Buratti, C., Barbanera, M., Palladino, D., 2014. An original tool for checking energy performance and certification of buildings by means of Artificial Neural Networks. Appl. Energy 120, 125–132.
Callejón-Ferre, A.J., Carreño-Sánchez, J., Suárez-Medina, F.J., Pérez-Alonso, J., Velázquez-Martí, B., 2014. Prediction models for higher heating value based on the structural analysis of the biomass of plant remains from the greenhouses of Almería (Spain). Fuel 116, 377–387.
Channiwala, S.A., Parikh, P.P., 2002. A unified correlation for estimating HHV of solid, liquid and gaseous fuels. Fuel 81, 1051–1063.
Chen, Q., Zhao, J., Vittayapadung, S., 2008. Identification of the green tea grade level using electronic tongue and pattern recognition. Food Res. Int. 41, 500–504.
Cordero, T., Marquez, F., Rodriguez-Mirasol, J., Rodriguez, J.J., 2001. Predicting heating values of lignocellulosics and carbonaceous materials from proximate analysis. Fuel 80, 1567–1571.
De, S., Kaiadi, M., Fast, M., Assadi, M., 2007. Development of an artificial neural network model for the steam process of a coal biomass cofired combined heat and power (CHP) plant in Sweden. Energy 32, 2099–2109.
Debdoubi, A., amarti, A.El, Colacio, E., 2005. Production of fuel briquettes from esparto partially pyrolyzed. Energy Convers. Manag. 46, 1877–1884.
Demirbaş, A., 1997. Calculation of higher heating values of biomass fuels. Fuel 76, 431–434.
Demirbaş, A., Ilten, N., 2004. Fuel analyses and thermochemical processing of olive residues. Energy Sources 26, 731–738.
Erol, M., Haykiri-Acma, H., Küçükbayrak, S., 2010. Calorific value estimation of biomass from their proximate analyses data. Renew. Energy 35, 170–173.
Filho, A.O.B., Barros, A.K.D., Labidi, S., Viegas, I.M.A., Marques, D.B., Romariz, A.R.S., de Sousa, R.M., Marques, A.L.B., Marques, E.P., 2015. Application of artificial neural networks to predict viscosity, iodine value and induction period of biodiesel focused on the study of oxidative stability. Fuel 145, 127–135.
Friedl, A., Padouvas, E., Rotter, H., Varmuza, K., 2005. Prediction of heating values of biomass fuel from elemental composition. Anal. Chim. Acta 544, 191–198.
Ghugare, S.B., Tiwary, S., Tambe, S.S., 2014. Computational intelligence based models for prediction of elemental composition of solid biomass fuels from proximate analysis. Int. J. Syst. Assur. Eng. Manag., 1–14
Giri, A.K., Patel, R.K., Mahapatra, S.S., 2011. Artificial neural network (ANN) approach for modelling of arsenic (III) biosorption from aqueous solution by living cells of Bacillus cereus biomass. Chem. Eng. J. 178, 15–25.
Goldfarb, J.L., Liu, C., 2013. Impact of blend ratio on the co-firing of a commercial torrefied biomass and coal via analysis of oxidation kinetics. Bioresour. Technol. 149, 208–215.
Guo, B., Li, D., Cheng, C., Lü, Z., Shen, Y., 2001. Simulation of biomass gasification with a hybrid neural network model. Bioresour. Technol. 76, 77–83.
Gupta, M., Jin, L., Homma, H. 2004. Static and Dynamic Neural Networks: From Fundamentals to Advanced Theory. John Wiley & Sons.
Haykiri-Acma, H., Yaman, S., Kucukbayrak, S., 2015. Does carbonization avoid segregation of biomass and lignite during co-firing? Thermal analysis study. Fuel Process. Technol. 137, 312–319.
Jenkins, B.M., Baxter Jr., L.L., Miles, T.R., 1998. Combustion properties of biomass. Fuel Process. Technol. 54, 17–46. T.R.M..
Jiménez, L., González, F., 1991. Study of the physical and chemical properties of lignocellulosic residues with a view to the production of fuels. Fuel 70, 947–950.
Kathiravale, S., Yunus, M.N.M., Sopian, K., Samsuddin, A.H., Rahman, R.A., 2003. Modeling the heating value of Municipal Solid Waste. Fuel 82, 1119–1125.
Küçükbayrak, S., Dürüs, B., Meríçboyu, A.E., Kadioglu, E., 1991. Estimation of calorific values of Turkish lignites. Fuel 70, 979–981.
Malik, M., Dincer, I., Rosen, M.A., 2015. Development and analysis of a new renewable energy-based multi-generation system. Energy 79, 90–99.
Masiá, A.A.T., Buhre, B.J.P., Gupta, R.P., Wall, T.F., 2007. Characterising ash of biomass and waste. Fuel Process. Technol. 88, 1071–1081.
Mason, D.M., Gandhi, K.N., 1983. Formulas for calculating the calorific value of coal and coal chars: Development, tests, and uses. Fuel Process. Technol. 7, 11–22.
Maurya, R., Ghosh, T., Paliwal, C., Shrivastav, A., Chokshi, K., Pancha, I., Ghosh, A., Mishra, S., 2014. Biosorption of methylene blue by de-oiled algal biomass: Equilibrium, kinetics and artificial neural network modelling. PLoS One 9.
McKendry, P., 2002. Energy production from biomass (part 1): overview of biomass. Bioresour. Technol. 83, 37–46.
Mesroghli, S., Jorjani, E., Chelgani, S.C., 2009. Estimation of gross calorific value based on coal analysis using regression and artificial neural networks. Int. J. Coal Geol. 79, 49–54.
Miranda, M.T., Arranz, J.I., Rojas, S., Montero, I., 2009. Energetic characterization of densified residues from Pyrenean oak forest. Fuel 88, 2106–2112.
Munir, S., Daood, S.S., Nimmo, W., Cunliffe, A.M., Gibbs, B.M., 2009. Thermal analysis and devolatilization kinetics of cotton stalk, sugar cane bagasse and shea meal under nitrogen and air atmospheres. Bioresour. Technol. 100, 1413–1418.
Nhuchhen, D.R., Salam, P.A., 2012. Estimation of higher heating value of biomass from proximate analysis: a new approach. Fuel 99, 55–63.
Parikh, J., Channiwala, S.A., Ghosal, G.K., 2007. A correlation for calculating elemental composition from proximate analysis of biomass materials. Fuel 86, 1710–1719.
Parikh, J., Channiwala, S.A., Ghosal, G.K., 2005. A correlation for calculating HHV from proximate analysis of solid fuels. Fuel 84, 487–494.
Patel, S.U., Kumar, B.J., Badhe, Y.P., Sharma, B.K., Saha, S., Biswas, S., Chaudhury, A., Tambe, S.S., Kulkarni, B.D., 2007. Estimation of gross calorific value of coals using artificial neural networks. Fuel 86, 334–344.
Principe, J.C., Euliano, N., Lefebvre, C. 2000. Neural and Adaptive Systems: Fundamentals through Simulations. John Wiley & Sons.
Ramadhas, A.S., Jayaraj, S., Muraleedharan, C., Padmakumari, K., 2006. Artificial neural networks used for the prediction of the cetane number of biodiesel. Renew. Energy 31, 2524–2533.
Sharifzadeh, M., Wang, L., Shah, N., 2015. Integrated biorefineries: CO2 utilization for maximum biomass conversion. Renew. Sustain. Energy Rev. 47, 151–161.

Shen, J., Zhu, S., Liu, X., Zhang, H., Tan, J., 2010. The prediction of elemental composition of biomass based on proximate analysis. Energy Convers. Manag. 51, 983–987.
Singh, A., Nigam, P.S., Murphy, J.D., 2011. Renewable fuels from algae: an answer to debatable land based fuels. Bioresour. Technol. 102, 10–16.
Suárez, J.A., Luengo, C.A., Felfli, F.F., Bezzon, G., Beatón, P.A., 2000. Thermochemical properties of cuban biomass. Energy Sources 22, 851–857.
Sugumaran, P., Seshadri, S., 2009. Evaluation of selected biomass for charcoal production. J. Sci. Ind. Res. (India) 68, 719–723.
Thipkhunthod, P., Meeyoo, V., Rangsunvigit, P., Kitiyanan, B., Siemanond, K., Rirksomboon, T., 2005. Predicting the heating value of sewage sludges in Thailand from proximate and ultimate analyses. Fuel 84, 849–857.
Vamvuka, D., Kakaras, E., Kastanaki, E., Grammelis, P., 2003. Pyrolysis characteristics and kinetics of biomass residuals mixtures with lignite. Fuel 82, 1949–1960.
Vani, S., Sukumaran, R.K., Savithri, S., 2015. Prediction of sugar yields during hydrolysis of lignocellulosic biomass using artificial neural network modeling. Bioresour. Technol. 188, 128–135.
Willis, M.J., Massimo, C.Di., Montague, G.A., Tham, M.T., Morris, A.J., 1991. Artificial neural networks in process engineering. IEE Proc. D – Control Theory Appl. 138, 256–266.
Xu, L., Yuan, J., 2015. Online identification of the lower heating value of the coal entering the furnace based on the boiler-side whole process models. Fuel 161, 68–77.
Yin, C.-Y., 2011. Prediction of higher heating values of biomass from proximate and ultimate analyses. Fuel 90, 1128–1132.